

High Isolation, Planar Filters Using EBG Substrates

William J. Chappell, *Member, IEEE*, Matthew P. Little, *Member, IEEE*, and Linda P. B. Katehi, *Fellow, IEEE*

Abstract—The concept of electromagnetic bandgaps (EBGs) has been utilized to develop a high-quality filter that can be integrated monolithically with other components due to a reduced height, planar design. Coupling adjacent defect elements in a periodic lattice creates a filter characterized by its ease of fabrication, high-*Q* performance, high-port isolation, and integrability to planar or 3-D circuit architectures. The filter proof of concept has been demonstrated in a metallocodielectric lattice. The measured and simulated results of 2-, 3-, and 6-pole filters are presented at 10.7 GHz.

Index Terms—Bandpass filters, electromagnetic bandgaps, high-*Q* planar filters, metallocodielectric lattices, photonic bandgaps.

I. INTRODUCTION

USING the concept of a constant coupling coefficient filter, a defect resonator is utilized to develop multipole filters that exhibit excellent insertion loss and isolation due to the high-*Q* exhibited by the electromagnetic bandgap (EBG) defect resonators [1]. The fabrication of these filters is extremely simple. It requires nothing more than via holes on a single substrate plane. Finally, since the EBG substrate prohibits substrate modes, the isolation between the input and output ports of the filter can be much greater than that of other planar filter architectures. Two, three, and six pole 2.7% filters were measured and simulated, with measured results showing insertion losses of -1.23 , -1.56 , and -3.28 dB, respectively. The out-of-band isolation was measured to be -32 , -46 , and -82 dB 650 MHz away from the center frequency (6% off center) for the three filters.

II. EBG FILTER CONCEPT

A high-*Q* resonator can be created in a periodic lattice of vias in a host dielectric substrate (a metallocodielectric EBG), by simply removing one of the periodic vias [1]. This defect mode was shown to have a *Q* that is nearly equivalent to a reduced height dielectric filled metal cavity, which is significantly greater than what can be achieved through other planar structures. The unloaded *Q* of the cavity is approximately 750, as implemented in this paper in Rogers Duroid 5880. Simulations show that the same configuration provides an unloaded *Q* above 1500 with the same configuration in an alumina substrate, while being nearly one third of the size. This resonator configuration allows the ability to create high-*Q* filters that can be mono-

Manuscript received February 6, 2001; revised April 16, 2001. This work was supported by the Low-Power Electronics MURI (Contract DAAH04-96-1-0377). The review of this letter was arranged by Associate Editor Dr. Arvind Sharma.

The authors are with the Radiation Laboratory, University of Michigan, Ann Arbor, MI 48109-2122 USA (e-mail: chappell@engin.umich.edu).

Publisher Item Identifier S 1531-1309(01)05428-9.

lithically fabricated utilizing a single substrate. In a previous filter attempt [2] only a single resonator was strongly coupled, which produces a highly unusable passband in both amplitude and group velocity. In contrast, in this paper, multiple resonators are coupled adjacently to create a usable passband as dictated by traditional filter theory. Other attempts have used nontraditional EBG concepts [3] but have not been proven to increase the *Q* over traditional half-wave resonators.

When the defect cavities are implemented adjacent to each other, the fields in the defects couple (as shown in Fig. 1). This coupling can be controlled to adjust the bandwidth of the filter. The external coupling of the filter can then be adjusted to critically couple to the resonators, which minimizes ripple and insertion loss. By controlling the two coupling parameters, interresonator coupling and external coupling, a narrowband bandpass filter has been developed out of the relatively high-*Q*, planar resonators.

III. COUPLING

A. Interresonator Coupling

The fields within a single defect resonator evanesce into the surrounding periodic lattice. As opposed to a more traditional enclosed cavity, the fields are not strictly localized within the defect region. When two defects are implemented adjacent to each other (as in Fig. 1), the fields in the defects couple. As the defects couple to each other, the central frequency peak of the single resonator separates into two distinct peaks. The amount that the peaks veer from their natural resonant frequency is a measure of the coupling coefficient. Therefore, Fig. 1 shows a graphical means in which to obtain the coupling coefficient between resonators. In order to discern distinct peaks in the transmission response, weak coupling to the defects is simulated. The coupling coefficient is then obtained and is related to the low-pass prototype values of the filter under development, by the following relations [4]:

$$k = \frac{f_1^2 - f_2^2}{f_1^2 + f_2^2} = \frac{BW}{\omega} \sqrt{\frac{1}{G_j G_{j+1}}} \quad (1.1)$$

where f_1 and f_2 are the frequencies of the peaks in S_{21} , while G_j , ω , and BW are the lowpass element value, the low-pass equivalent cutoff, and bandwidth of the filter, respectively.

The sidewalls of the metallocodielectric resonator may be interpreted as a high-pass, two-dimensional (2-D) spatial filter comprised of many periodic short evanescent sections. The rejection of the high pass filter created by the evanescent sections defines the confinement of the fields, and therefore the coupling between adjacent resonators. This rejection is determined by the spacing between the rods that make up the short evanescent sections. The further apart the metal surfaces of the vias that define

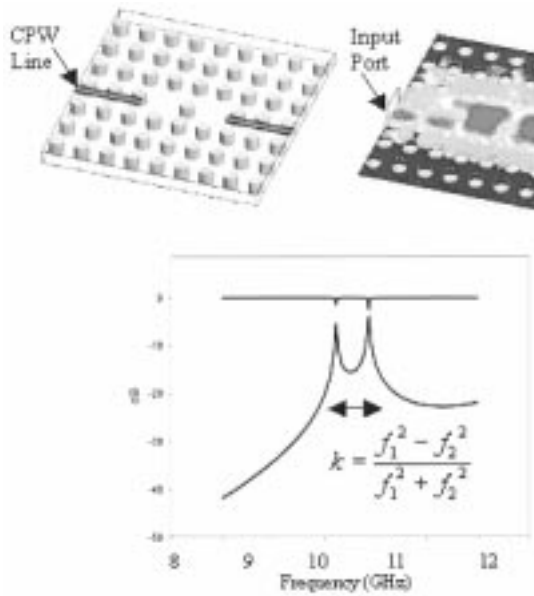


Fig. 1. Two-pole simulation and electric field plot of coupled defects determining interresonator coupling.

the sidewalls of the resonators are from each other, the less the field surrounding the defect region evanesces. Therefore, by decreasing the size of the radius of the rod or by increasing the lattice period, the coupling increases. As the coupling between the defects becomes greater, the bandwidth of the filter increases as well.

B. External Coupling

In addition to the internal coupling, the external coupling Q_e must be designed to control the overall insertion loss and ripple in a multipole filter. The desired external coupling for the given coupled resonators is given as

$$Q_c = \frac{G_0 G_1 \omega}{BW}. \quad (1.2)$$

This external coupling can be extracted using simulated values of a single defect resonator. The coupling mechanism may be adjusted resulting in an altered loaded Q_1 of the system. Since the unloaded Q_u of the resonator has already been obtained for a single resonator, the external Q can be extracted from the relation

$$\frac{1}{Q_1} = \frac{1}{Q_u} + \frac{1}{Q_e}. \quad (1.3)$$

A simulation on a single resonator provides the 3-dB width for a given coupling scheme and, therefore, extracts the loaded Q value, which in turn determines the external Q .

For the metallocodielectric filter described herein, a CPW line is used to provide the necessary external coupling as shown in Fig. 1. The CPW line, printed on the top of the substrate, is fed through the metallic lattice, probing into the defect cavity. The further the CPW line probes into the cavity, the lower the value of the external Q_e . If the external Q_e is too high, then distinct peaks are observed as large ripples in the transmission response. For this undercoupled case, the CPW line should be moved further into the cavity to lower the external Q_e .

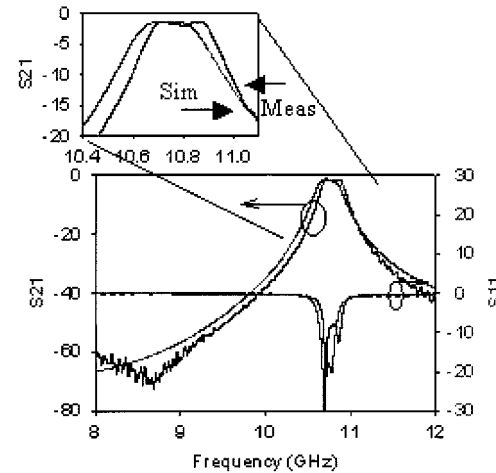


Fig. 2. Two pole filter-simulated versus measured.

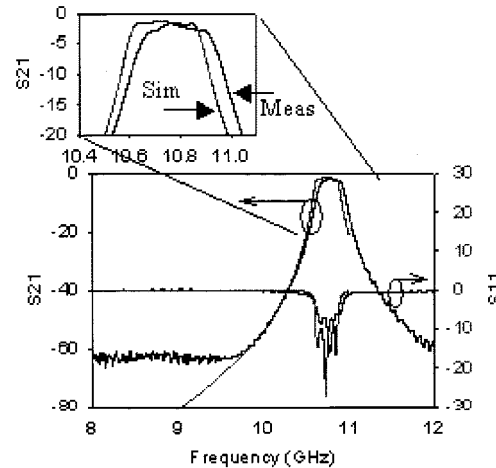


Fig. 3. Three pole filter-simulated versus measured.

IV. FILTER REALIZATION

Using the concepts described above to control the coupling of the resonators, a prototype filter was developed out of Duroid 5880, $\epsilon_r = 2.2$, loss tan = 0.0009. The filter has a center frequency at 10.7 GHz with approximately a 2.7 % bandwidth. Using a full-wave simulation of a two resonator substrate [Ansoft HFSS FEM software], the diameter of the rods and the lattice period were adjusted to provide the correct coupling coefficients to provide the desired 2.7% bandwidth. Then, the length of the CPW line was adjusted to critically couple the filter to provide minimum insertion loss.

The resulting lattice has a transverse period of 9 mm, longitudinal period of 7 mm, and rod radius of 2 mm. For a substrate height of 120 mils, the unloaded Q of this resonator is ~ 750 . For critical coupling for these via spacings, the CPW line is shorted 3 mm into the first and last defect. A total of five periods of vias (two on each side of the resonator) is needed to constrain the fields within the resonators and produce a negligible leakage loss. While the total area is larger than a half wave microstrip resonator filter, it has substantially better Q performance. In comparison to an equivalent dielectric filled, reduced height metallic cavity, the defect region itself is smaller due to the inductive nature of the defining sidewalls (14 mm \times 10 mm versus

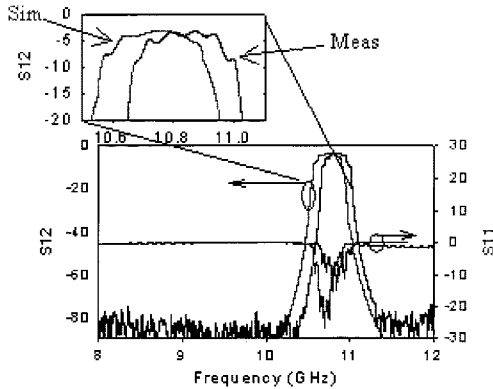


Fig. 4. Six pole filter—simulated versus measured.

TABLE I
COMPARISON OF THE MEASURED AND
SIMULATED FILTER DATA

Filter	Center Freq. (GHz)	Insertion Loss (dB)	Band Width (GHz)	Isolation 6 % off center
2-Pole Sim	10.727	-1.37	0.263	-32 dB
2-Pole Meas	10.787	-1.23	0.265	-30 dB
3-Pole Sim	10.73	-1.32	0.290	-42 dB
3-Pole Meas	10.797	-1.56	0.293	-45 dB
6-Pole Sim	10.725	-3.26	0.279	> -100 dB
6-Pole Meas	10.8275	-3.28	0.257	-80 dB

15 mm × 12 mm). The overall structure of the filter is larger than an equivalent metallic cavity filter with solid sidewalls, though, because of the multiple layers of vias needed. However, this method provides integrability to the rest of the planar circuitry and an ease of fabrication that a traditional cavity filter does not.

These same lattice parameters were used in cascaded stages to create multiple pole filters by introducing multiple adjacent defects. A three-pole and a six-pole filter were developed with the goal of an optimal insertion loss relative to a maximum out of bandwidth isolation. By not altering the lattice parameters for the different stages of defects, a constant coupling coefficient filter was constructed, with equivalent lowpass elements

$$G_0 = G_1 = G_2 = \dots = G_n = 1. \quad (1.4)$$

It is stated in [5] that this constant coupling coefficient configuration gives an optimal insertion loss for a given out-of-band isolation. The results can be seen in the plots of Figs. 2–4 and can be numerically compared in the Table I included at the end of this paper.

The measurements and simulations compare favorably. The resonant frequency agrees within 1% in all cases (0.5% in the two pole filter, 0.7% for the three pole filter, and 0.8% in the six pole filter). The slight shift in frequency is due to the fact that the FEM model used cannot accurately model complete circles and

must approximate them as polygons. Therefore the vias have been simulated slightly different than what was measured. The bandwidth is nearly exact for the 2 and 3 pole filters (< 1% difference) but is 23 MHz less for the measured six-pole filter. The difference in bandwidth for the six-pole filter is the result of the hand placement of the feed lines relative to the lattice of vias. Due to the misalignment, the measured filter is not exactly critically coupled. The outside poles in the measured response are so weakly coupled that they do not factor in the pass-band bandwidth. Also evident in the comparison is the increased ripple in the pass band of the measured filters. The ripple is also caused by weak external coupling to the filters. The out of band isolation was excellent, due to the fact that the substrate does not support substrate modes. For the six-pole filter, the transmission reached the noise floor 4.3% away from the center frequency. The out-of-band isolation is limited by the space wave coupling of the CPW lines, which can be eliminated by packaging the CPW lines, placing a reflective boundary or absorber between the ports, or fabricating the CPW lines on opposite sides of the substrate. Note that the measured results were achieved without tuning any of the parameters, nor were any of the losses of the connectors or feed lines deembedded.

V. CONCLUSION

In conclusion, a relatively simple, high-*Q* filter was measured, simulated, and analyzed with good agreement and without the need for tuning. High isolation relative to other planar filters was obtained since substrate noise is eliminated using the properties of the EBG substrate. A low insertion loss was obtained due to the low loss nature of the resonators. The relatively high-*Q* performance is superior to what could be obtained in other planar architectures. The EBG/via hole architecture makes these filters amenable to planar circuit integration. More advanced geometries and materials are expected to make these filters smaller with even better performance in future applications.

REFERENCES

- [1] W. J. Chappell, M. P. Little, and L. P. B. Katehi, "High *Q* two dimensional defect resonators—Measured and simulated," in *IEEE MTT-S Conf.*, Boston, MA, June 2000.
- [2] M. J. Hill, R. W. Ziolkowski, and J. Papapolymerou, "Simulated and measured results from a duroid-based planar MBG cavity resonator filter," *Microwave Guided Wave Lett.*, vol. 10, pp. 528–530, Dec. 2000.
- [3] F. R. Yang, K. P. Ma, and Y. X. Qian *et al.*, "A uniplanar compact photonic bandgap (UC-PBG) structure and its application for microwave circuits," *IEEE Trans. Microwave Theory Tech.*, vol. 47, pp. 1509–1514, Aug. 1999.
- [4] A. Brown, "High-*Q* integrated micromachined components for a 28-GHz front-end receiver," Ph. D., dissertation, Univ. Michigan, Ann Arbor, 1999.
- [5] G. L. Matthei, L. Young, and E. M. T. Jones, *Microwave Filters, Impedance Matching Networks, and Coupling Structures*. Norwell, MA: Artech House, 1980.